

Polarization stabilization of vector solitons in circularly birefringent fibers induced by Raman effect.

E.A.Kuzin^a, B.A.Villagomez-Bernabe^a, N.Korneev^a, B.Ibarra-Escamilla^a, A. Gonzalez- Garcia^a, O.Pottiez^b,
M. Duran-Sanchez^c

^aInstituto Nacional de Astrofísica, Óptica y Electrónica, Santa Ma. Tonantzintla, Puebla, México,

^bCentro de Investigaciones en Óptica, Leon, Gto. México,

^cUniversidad Tecnológica de Puebla, Puebla, Mexico.

ABSTRACT

Common optical fibers are randomly birefringent, and solitons traveling in them develop random polarization states upon propagation. However it is desirable to have solitons with a well-defined polarization. We analyzed the two coupled propagation equations in a circularly birefringent fiber. Our equations included the soliton self frequency shift. For our best knowledge this set of equation was analyzed for the first time. We performed a transformation of equations which reduces them to a form of perturbed Manakov task. The difference between our equations and the integrable Manakov case was considered as a perturbation. The perturbation method gives us an equations for evolution of the polarization state of pulse. The evaluation equation shows that in a circularly birefringent (twisted) fiber the cross-polarization Raman term leads to unidirectional energy transfer from the slow circularly polarized component to the fast one. The magnitude of this effect is determined by the product of birefringence and amplitudes of both polarization components. Thus, solitons with any initial polarization state will eventually evolve stable circularly polarized solitons. We also solved equations using a split-step Fourier method. The parameters of a standard fiber were used with delay between left- and right- circular polarizations of 1 ps/km that corresponds a fiber twisted by 6 turns/m.

Keywords: Soliton, Raman scattering, birefringence.

1. INTRODUCTION

Soliton propagation in optical fiber is often treated as a scalar problem, and the vector nature of light is ignored [1]. Common optical fibers, however, are randomly birefringent, and pulses traveling in them develop random polarization states upon propagation. The propagation of a pulse in a low birefringence fiber was considered for the first time in [2–4] using coupled nonlinear Schrödinger equations. It was shown that fractional pulses in each of the two polarizations trap each other and move together as one unit called vector soliton. The frequency of each pulse is shifted to compensate the difference in group velocities caused by birefringence. The experimental observation of vector solitons was reported in [5].

Attention was given mainly on the vector solitons in linearly birefringent fibers; the effect of the Raman soliton self-frequency shift and circularly birefringent fibers, as far as we know, were never considered. However, fibers with circular birefringence, in particular twisted ones, may present advantages for laser applications. Fiber twist introduces circular birefringence and cancels random linear birefringence [6]. This makes the twisted fiber less sensitive to environmental conditions and provides new useful features for nonlinear applications [7].

In this paper we demonstrate that in a circularly birefringent fiber the cross-polarization Raman term leads to unidirectional energy transfer from the slow circularly polarized component to the fast one. The magnitude of this effect is determined by the product of birefringence and amplitudes of both polarization components. Thus, solitons with any initial polarization state will eventually evolve in a twisted fiber into stable circularly polarized ones. We demonstrate this effect numerically and make an analytic estimation of its magnitude using a perturbation theory for vector solitons [8].

2. THEORY

The equations that describe self frequency shift a pulse with linear polarization usually are written as follows [9]:

$$\partial_z A_x = i\gamma [T_R \partial_T |A_x|^2] A_x, \quad (1)$$

$$\partial_z A_y = i\gamma [T_R \partial_T |A_y|^2] A_y. \quad (2)$$

Here A_x and A_y are the envelopes of the pulse with linear polarization of both x and y axes, γ is the nonlinearity and T_R is the Raman response time.

However, experimental results [10] show that Raman gain caused by perpendicular component also may be important especially for small Raman shift so for self frequency shift the following equations have to be used:

$$\partial_z A_x = i\gamma [T_R \partial_T |A_x|^2] A_x + i\alpha\gamma [T_R \partial_T |A_y|^2] A_x, \quad (3)$$

$$\partial_z A_y = i\gamma [T_R \partial_T |A_y|^2] A_y + i\alpha\gamma [T_R \partial_T |A_x|^2] A_y. \quad (4)$$

Here $\alpha = \alpha_{\perp}/\alpha_{\parallel}$ where α_{\perp} and α_{\parallel} denote, respectively, the perpendicular and parallel Raman gains.

Using circularly polarized components defined as

$$A_+ = (A_x + iA_y)/\sqrt{2}, \quad (5)$$

$$A_- = (A_x - iA_y)/\sqrt{2}. \quad (6)$$

The A_+ and A_- represent right- and left-handed circularly polarized states, respectively. Introducing Eqs. 5 and 6 into Eqs. 3 and 4 we have the following equations:

$$\partial_z (A_+ + A_-) = \frac{i\gamma T_R}{2} (A_+ + A_-) \partial_t (|A_+ + A_-|^2) + \frac{i\alpha\gamma T_R}{2} (A_+ + A_-) \partial_t (|A_+ - A_-|^2), \quad (7)$$

$$\partial_z (A_+ - A_-) = \frac{i\gamma T_R}{2} (A_+ - A_-) \partial_t (|A_+ - A_-|^2) + \frac{i\alpha\gamma T_R}{2} (A_+ - A_-) \partial_t (|A_+ + A_-|^2). \quad (8)$$

If we sum Eqs. 7 and 8 we can obtain the equation for the right circularly polarized state as follows:

$$\partial_z A_+ = \frac{i\gamma T_R}{2} \left\{ \frac{1+\alpha}{2} \partial_t (|A_+|^2 + |A_-|^2) A_+ + (1-\alpha) \partial_t [Re(A_+ A_-^*)] A_+ \right\}. \quad (9)$$

Similarly if we subtract equations 7 and 8 we can obtain the equation for the left circularly polarized state as follows:

$$\partial_z A_- = \frac{i\gamma T_R}{2} \left\{ \frac{1+\alpha}{2} \partial_t (|A_+|^2 + |A_-|^2) A_- + (1-\alpha) \partial_t [Re(A_+ A_-^*)] A_+ \right\}. \quad (10)$$

Equations 9 and 10 are a equations coupling system for SRS phenomenon. Adding GVD and walk-off between circularly polarized components, SPM and XPM terms to these equations we have [11]:

$$\partial_z A_+ + \beta_1 \partial_t A_+ + \frac{i\beta_2}{2} \partial_t^2 A_+ = \frac{2i\gamma}{3} (|A_+|^2 + 2|A_-|^2) A_+ - \frac{i\gamma T_R}{2} \left\{ \frac{1+\alpha}{2} \partial_t (|A_+|^2 + |A_-|^2) A_+ + (1-\alpha) \partial_t [Re(A_+ A_-^*)] A_- \right\}, \quad (11)$$

$$\partial_z A_- - \beta_1 \partial_t A_- + \frac{i\beta_2}{2} \partial_t^2 A_- = \frac{2i\gamma}{3} (|A_-|^2 + 2|A_+|^2) A_- - \frac{i\gamma T_R}{2} \left\{ \frac{1+\alpha}{2} \partial_t (|A_+|^2 + |A_-|^2) A_- + (1-\alpha) \partial_t [Re(A_+ A_-^*)] A_+ \right\}. \quad (12)$$

The last two terms of left side are walk-off and GVD respectively. The terms in parenthesis of right side are SPM and XPM terms. Finally the terms in key are the SRS terms.

The vector soliton can be approximated by the form (not taking into account phases)

$$|A_+(z)| = A \cos(\theta) \operatorname{sech} \left[A(t - t_0) / \sqrt{|\beta_2|} \right], \quad (13)$$

$$|A_-(z)| = A \cos(\theta) \operatorname{sech} \left[A(t - t_0) / \sqrt{|\beta_2|} \right]. \quad (14)$$

Using Eqs. 13 and 14 we can define the ratio between powers of circularly left- and right-polarized components as follows [11]:

$$\frac{|A_-(z)|}{|A_+(z)|} = \tan(\theta(0)) \exp \left[\frac{2(1-\alpha)}{3} \gamma A^2 \frac{T_R \beta_1}{|\beta_2|} z \right]. \quad (15)$$

3. NUMERICAL RESULTS

Equations 11 and 12 were resolved using the split-step Fourier method [7]. The values of using parameters are: $\beta_1=1$ ps/km; $\beta_2=-25$ ps²/km; $\alpha=0.3$; $\gamma=1.6$ 1/(W-km); $T_R=3$ fs. For simulations we introduced the 30-ps, 40-W pulse in the fiber. The Gaussian noise was imposed on the pulse. Modulation instability breaks up the pulse into a set of solitons. We tracked the highest soliton in this set.

Fig. 1 shows the influence of walk-off between circularly right- and left-polarized components on ellipticity for a soliton with linear polarization at the entrance. The fiber optic length varies from 0.8 km to 1.2 km. Fig. 2a shows that without twist in the fiber ($\beta_1=0$), ellipticity keeps constant inside the fiber, nevertheless Fig. 2b shows that in the twisted fiber ($\beta_1=1$) the soliton ellipticity increases along the fiber. Note that in the last case the ellipticity of the highest soliton does not coincide with the ellipticity of the input pulse.

Making simulations with random noise imposed on the input pulse we have found that the ellipticity of the highest soliton is distributed randomly about the ellipticity of the input pulse. Fig. 2 shows the results of five simulations each with different random noise at the entrance pulse. We can see that solitons appear with different ellipticity distributed around the ellipticity of the input pulse. However ellipticity of all solitons grows at the propagation along the fiber. The growth of the ellipticity means that the ratio between the amplitudes of the right- and left-circularly polarized component grows. For our equations the right-circularly polarized component is fast one. So the polarization approaches to the fast circularly polarized component.

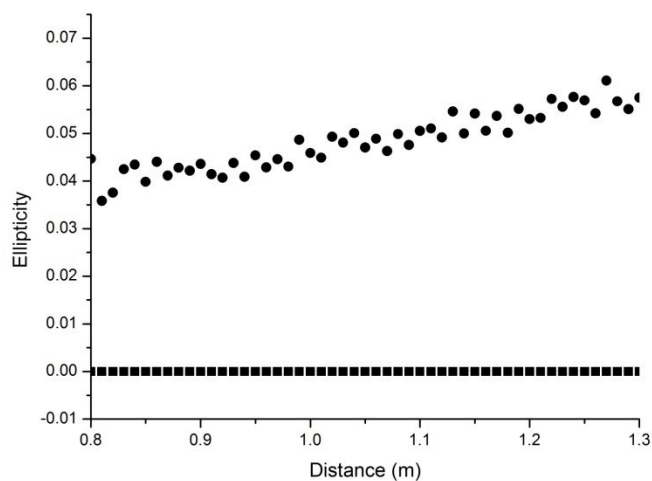


Figure 1. Ellipticity vs fiber length for a soliton with linearly polarized pulse at the entrance for $\beta_1=1$ (circles) and $\beta_1=0$ (squared).

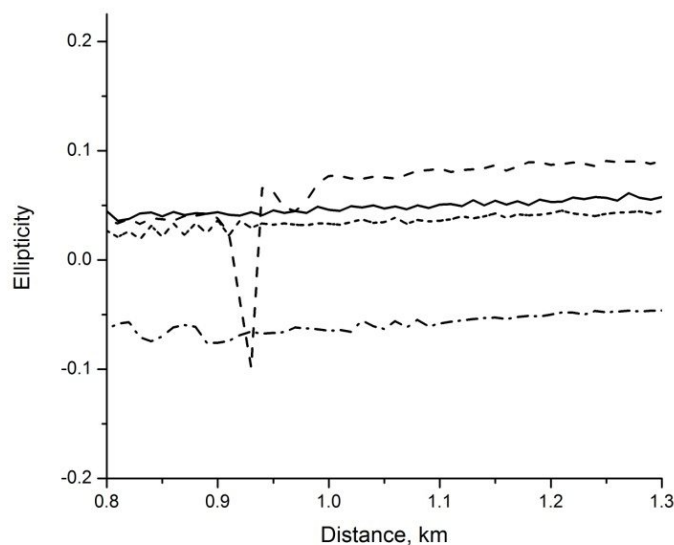


Figure 2. Ellipticity vs fiber length for five simulations with different noise for a soliton generated from the linearly polarized pulse at the entrance using $\beta_1=1$.

The change of the sign of β_1 results in the decrease of the ellipticity that means the increase of the ratio between left- and right-circularly polarized components. Figure 3 shows the results the positive and negative β_1 . For negative β_1 the left circularly polarized component is fast one. We can see that for both cases the polarization moves to fast circularly polarized component. The value and the sign of the coefficient β_1 are defined by the fiber twist; our particular value of coefficient β_1 corresponds to the fiber twist of 6 turn/m. For elliptical polarization we found the same behavior of the polarization ellipticity that shows the energy transform from the slow to fast circularly polarized component.

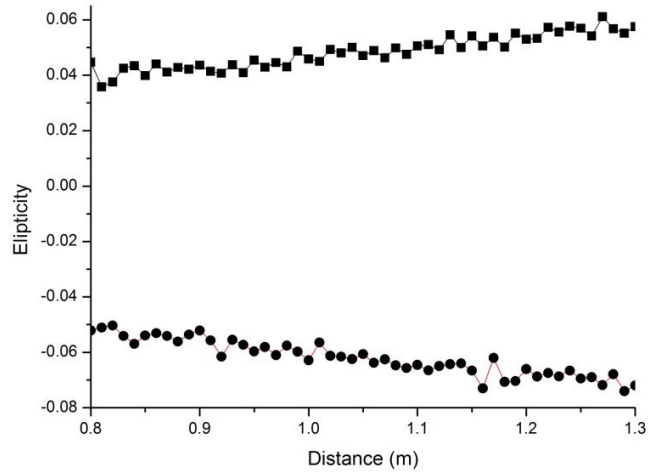


Figure 3. Ellipticity vs fiber length for solitons generated from the pulse with linear ellipticity at the entrance for $\beta_1=-1$ (circles) and $\beta_1=1$ (squared).

The generation of solitons in the process of MI is stochastic process. We calculated the ellipticity of solitons generated in the process of MI for different noise imposed on the input pulse. The ellipticity of the highest solitons was found to be randomly distributed around the polarization of the input pulse. Figure 4 shows the number of solitons appeared with different ellipticity when linearly polarized input pulse was used. As we can see solitons with wide range of the polarization ellipticity can appear.

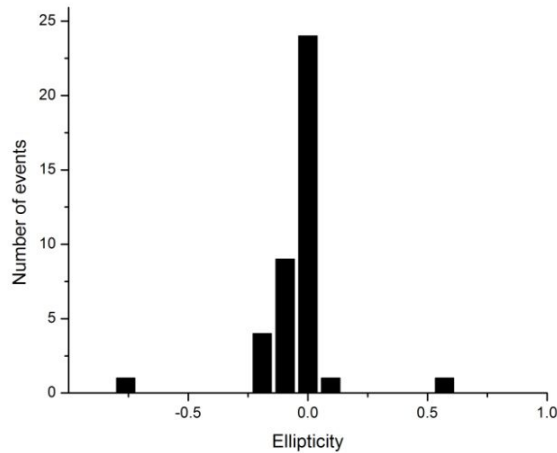


Figure 4. The number of solitons with different ellipticity generated by MI at linear polarization of the input pulse.

At polarization of the input pulse close to circular the dispersion of the polarization ellipticity of solitons is much less, see Fig. 5 and Fig. 6. The polarization ellipticity of the input pulse was equal to 0.98 for Fig. 5 and -0.98 for Fig. 6. We can see that most of solitons have the ellipticity closer to circular polarization that the input pulse.

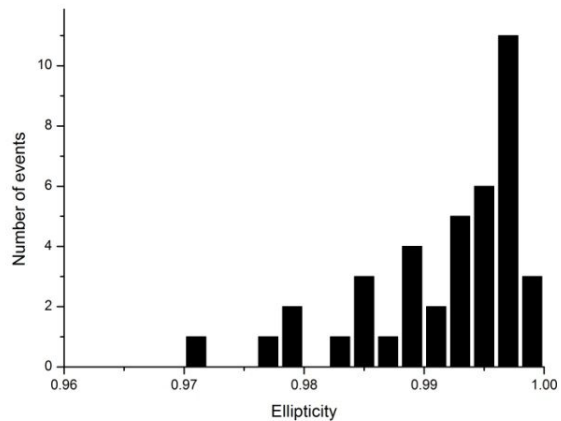


Figure 5. The number of solitons with different ellipticity generated by MI at polarization of the input pulse close to circular.

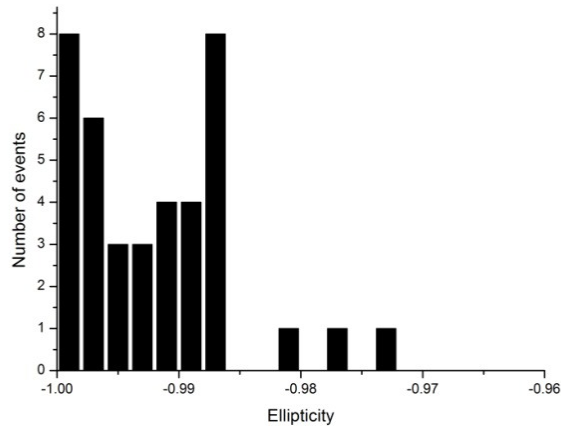


Figure 6. The number of solitons with different ellipticity generated by MI at polarization of the input pulse close to circular.

4. CONCLUSIONS

We demonstrated numerically and by analytical analysis that in a fiber with circular birefringence the joint action of the Raman self-frequency shift and group velocity difference between left- and right-circularly polarized components results in the unidirectional energy transfer from the slow circularly polarized component to the fast one. The magnitude of this effect is determined by the product of birefringence and amplitudes of both polarization components. Thus, solitons with any initial polarization state will eventually evolve into the stable circularly polarized ones.

5. ACKNOWLEDGMENT

This work was supported by the CONACYT project 130966.

REFERENCES

- [1] Mollenauer, L.F., Stolen R.H. and Gordon J.P., "Experimental observation of picoseconds pulse narrowing and solitons in optical fiber," *Phys. Rev. Lett.* 45(13), 1095-1098 (1980).
- [2] Menyuk, C.R., "Stability of solitons in birefringent optical fibers. **I**: Equal propagation amplitudes," *Opt. Lett.* 12(8), 614-616 (1987).
- [3] Menyuk, C.R., "Stability of solitons in birefringent optical fibers. **II**. Arbitrary amplitudes," *J. Opt. Soc. Am. B* 5(2), 392-402 (1988).
- [4] Christodoulides, D.N. and Joseph, R.I., "Vector solitons in birefringent nonlinear dispersive media," *Opt. Lett.* 13(1), 53-55 (1988).
- [5] Islam, M. N., Poole C. D. and Gordon J. P., "Soliton trapping in birefringent optical fibers," *Opt. Lett.* 14(18), 1011-1013 (1989).
- [6] Tsao, Ch., *Optical fiber waveguide analysis* (Oxford University Press, New York, 1999).
- [7] Tanemura, T. and Kikuchi K., "Circular-birefringence fiber for nonlinear optical signal processing," *J. Lightwave Technol.* 24(11), 4108-4119 (2006).
- [8] Midrio, M., Wabnitz S. and Franco P., "Perturbation theory for coupled nonlinear Schrödinger equations," *Phys. Rev. E.*, 54(5), 5743-5751 (1996).
- [9] Agrawal, G. P., [Nonlinear Fiber Optics], Academic Press, 48-49 (2001).
- [10] Mandelbaum, I., Bolshtyansky, M., Heinz, F., Hight, R., "Method for measuring gain tensor in optical fibers," *J. Opt. Soc. Am. B.* 23(4), 621-627 (2006).
- [11] Korneev, N., Kuzin, E. A., Villagomez-Bernabe, B. A., Pottiez, O., Ibarra-Escamilla, B., González-García, A., Durán-Sánchez, M., "Raman-induced polarization stabilization of vector solitons in circularly birefringent fibers," *Optics Express* 20(22), 24289 (2012).